

Dissipative Hydrodynamics of Rigid Spherical Particles

Albert S. Kim^{1,2}

¹*Civil and Environmental Engineering, University of Hawaii at Manoa, Honolulu, Hawaii 96822, USA*

²*Chemical Engineering, Kyung Hee University, Gyeonggi-do 449-701, Korea*

(Received May 14, 2012; CL-120528; E-mail: albertsk@hawaii.edu)

A unified version of particle dynamics simulation, dissipative hydrodynamics (DHD), is proposed by selecting advantageous features of Brownian dynamics, Stokesian dynamics, and dissipative particle dynamics. A stochastic differential equation is adopted as a governing equation, and the Ito–Wiener process is incorporated to fundamentally deal with the fluctuation theorem. As a result, DHD developed in this study is free from the typical restriction that the time interval should be considerably longer than the particle relaxation time.

In applied science and engineering disciplines, dynamic simulations of particulate materials are important in investigating microscopic phenomena. In the aqueous phase, a difficulty in particle dynamics simulation stems from the finite sizes of particles, which creates the volume exclusion interaction. Conventional molecular dynamics (MD) treats ions as interacting point particles and updates particle positions and velocities (at time t) of ions to those in the future (at time $t + dt$), given exerted ionic/external forces. A specific analysis of particle history can provide macroscopic quantities, which may be compared with experimental observations. In this case, the choice of time step dt must be considerably *smaller* than the typical time for a molecule to travel the length of its diameter.

When solute motion is of greater interest for a statistical mechanical analysis, the solvent molecular motion can be omitted in MD simulations and further replaced by random and frictional forces on solutes. Then, the governing equation switches from the Newton equation to Langevin equation, for which the time integration is standard Brownian dynamics (BD) simulation. Unlike MD, the time step dt in BD is supposed to be considerably *longer* than the particle relaxation time, defined as $\tau = m/\xi$, where m is the particle mass and ξ is the drag force coefficient. In a unit relaxation time, a sufficient number of particle collisions with a number of solvent molecules must occur, resulting in random drifting of the particles. Although ξ is proportional to the particle size, BD adopts the Oseen tensor and treats particles (like MD) as zero-size masses. Therefore, volume exclusion is often disregarded.^{1,2}

The lubrication tensors of Stokesian dynamics (SD) include the volume exclusion forces at a macroscopic level. A many-body far-field grand mobility matrix is built using the pair-wise superposition of the two-body mobility matrix. SD updates the many-body diffusion tensor from that of BD with much higher accuracy and rigor. The Langevin equation is the common governing equation for BD and SD so that both methods are intrinsically subject to the basic restriction of relaxation time: $dt \gg \tau$. Most of the SD simulations are limited to (presumed) zero inertia so that only drifting motion was investigated under conservative/external force fields.

Dissipative particle dynamics (DPD) fundamentally resolves the restrictive condition by incorporating the Fokker–Planck equation with the Ito–Wiener process. The stochastic differential equation (SDE) was used as a governing equation, and the accuracy of many-body hydrodynamic interactions in DPD is between BD and SD. Hydrodynamic resistances are presumed to be pair-wise resistances and described as (intuitively chosen) simple functions of the distance (r) between the two identical spheres: $\omega_D = \omega_R^2 = (1 - r/r_c)^2$ for $r < r_c$, where r_c is the cutoff distance above which $\omega_D = \omega_R = 0$.^{3,4}

Table 1 summarizes specific features of above-discussed simulation methods. Only MD uses the Newton equation as a governing equation, and BD/SD and DPD/DHD use the Langevin and stochastic differential equations, respectively. Because the dynamic simulation requires the integration of the second-order ordinary differential equation with respect to time, the inclusion of inertia (acceleration) in the simulations is a major task, which is not often studied in SD. All the simulation methods can surely include effects of conservative and/or external force fields. Brownian motion and multibody hydrodynamic forces are most accurately implemented in SD and DHD. More importantly, our DHD is the only simulation method for many-body hydrodynamics, which is not subject to the time interval restriction, and therefore, shows a promising potential to accurately and rigorously investigate microscopic phenomena such as systems of confined Brownian particles.

In this work, we aim to develop a unified particle dynamics method, called dissipative hydrodynamics (DHD) by selecting advantageous features of BD, SD, and DPD for accurate hydrodynamics without the time interval restriction. DHD adopts the SDE (from DPD) and the rigorous hydrodynamics (from SD) to investigate translational and rotational motion of N particles at an ambient temperature T :

$$\mathbf{M} \cdot d\mathbf{v} = (\mathbf{Q}^p - \mathbf{R} \cdot \Delta \mathbf{v}) dt + \mathbf{B} \cdot d\mathbf{W} \quad (1)$$

where \mathbf{M} is the mass/moment-of-inertia matrix of $6N \times 6N$ dimension; $\Delta \mathbf{v} = \mathbf{v} - \mathbf{V}^\infty$, the translational/rotational particle velocity \mathbf{v} relative to the fluid velocity \mathbf{V}^∞ ; \mathbf{Q}^p , the conservative force/torque vector of the same dimension as $\Delta \mathbf{v}$; \mathbf{R} , the $6N \times 6N$ grand resistance matrix; \mathbf{B} , the Brownian matrix (defined in this study) of zero mean and finite variance, i.e., $\langle \mathbf{B} \rangle = 0$ and $\langle \mathbf{B}^{\text{tr}} \cdot \mathbf{B} \rangle = 2k_B T$ (k_B is the Boltzmann constant); and $d\mathbf{W}$, the Ito–Wiener process of $6N$ elements. In the above SDE (1), $dW_k^{(i)}$ of particle i has six components for three-dimensional translational ($k = 1-3$) and rotational ($k = 4-6$) motion and has the following mathematical properties: (i) $W_k^{(i)}(t = 0) = 0$, (ii) $W_k^{(i)}(t)$ is continuous, (iii) $dW_k^{(i)} \equiv W_k^{(i)}(t + \delta t) - W_k^{(i)}(t)$ follows the normal distribution, and finally, (iv) $dW_k^{(i)} \cdot dW_k^{(i)} = dt$ for each translation and rotation. For mathematical simplicity, the Ito–Wiener process is normalized as $\mathbf{w} = d\mathbf{W}/\sqrt{dt}$.

Table 1. Comparison of dynamic simulation methods^a

| | MD | BD | SD | DPD | DHD |
|---------------|----------------------|-----------------------------|-----------------------------|----------------------|----------------|
| Govern. Eq. | Newton | Langevin | Langevin | SDE | SDE |
| Acceleration | ✓ | ✓ | possible | ✓ | ✓ |
| Conservative | ✓ | ✓ | ✓ | ✓ | ✓ |
| Brownian | × | simple | rigorous | approx. | rigorous |
| Hydrodynamic | × | constant | accurate | pair-wise | accurate |
| Time interval | subject to algorithm | restricted to $dt \gg \tau$ | restricted to $dt \gg \tau$ | subject to algorithm | not restricted |

^aCapability and incapability of each dynamics method (for specific aspects in the left column) are indicated by ✓ and ×, respectively.

The Brownian matrix \mathbf{B} can be calculated by decomposing the grand resistance matrix: $\mathbf{R} = \mathbf{A}^{\text{tr}} \cdot \mathbf{A} = \mathbf{A}^{\text{tr}} \cdot \mathbf{I} \cdot \mathbf{A}$ where \mathbf{A}^{tr} is a transpose of \mathbf{A} , and \mathbf{I} is the identity matrix, which is statistically represented as $\mathbf{I} = \langle \mathbf{C}^{\text{tr}} \cdot \mathbf{C} \rangle$ using a random row vector \mathbf{C} of $6N$ elements with zero mean and unit variance. We define $\mathbf{B} = \sqrt{2k_{\text{B}}T} \mathbf{C} \cdot \mathbf{A}$ and rewrite eq 1 as $\mathbf{M} \cdot d\mathbf{v} = \mathbf{Q} dt$ where \mathbf{Q} is the generalized force/torque vector: $\mathbf{Q} = (\mathbf{Q}^p - \mathbf{R} \cdot \Delta\mathbf{v}) + \mathbf{B} \cdot \mathbf{w} / \sqrt{dt}$. If the inertia is neglected in the absence of the conservative forces/torques, the velocity is simply $\mathbf{v} = \mathbf{V}^{\infty} + \mathbf{R} \cdot \mathbf{B} \cdot \mathbf{w} / \sqrt{dt}$, as influenced by only convective and diffusive transport of solvents, and the future translational/rotational position is represented as $\mathbf{r}(t + dt) = \mathbf{r}(t) + d\mathbf{r}$ where $d\mathbf{r} = \mathbf{v}(t) dt$. Note that $d\mathbf{r}$ is proportional to \sqrt{dt} .

To rigorously describe the configuration-dependent hydrodynamic drag tensors and rapidly fluctuating random stochastic forces/torques, we restrict ourselves to hard sphere systems by discarding interparticle interactions. As the inertia is often neglected in SD due to the time interval restriction ($dt \gg \tau$), we fundamentally resolve the restriction by adopting the SDE and Ito–Wiener process to maintain a simulation accuracy similar to that for SD. A simple time integration using an intermediate time step is adopted from standard DPD algorithms:⁵

$$v(t') = v(t) + \mathbf{R}(t) \cdot \mathbf{Q}(t) \left[\frac{1}{2} dt \right] \quad (2)$$

$$r(t') = r(t) + v(t) \left[\frac{1}{2} dt \right] + \frac{1}{2} \mathbf{R}(t) \cdot \mathbf{Q}(t) \left[\frac{1}{2} dt \right]^2 \quad (3)$$

$$v(t + dt) = v(t') + \mathbf{R}(t') \cdot \mathbf{Q}(t') \left[\frac{1}{2} dt \right] \quad (4)$$

$$r(t + dt) = r(t') + v(t') \left[\frac{1}{2} dt \right] + \frac{1}{2} \mathbf{R}(t') \cdot \mathbf{Q}(t') \left[\frac{1}{2} dt \right]^2 \quad (5)$$

where $dt^2 = (dt)^2$ and $t' = t + 0.5dt$. $\mathbf{R}(t')$ and $\mathbf{Q}(t')$ indicates that they are evaluated at time t' with $r(t')$ and $v(t')$ evaluated at time t . The use of half-step evolution is critical in this dissipative system since the drag force/torque changes its direction following the sign of relative translational/rotational velocities. Otherwise, particles must engage in unrealistic oscillatory motion, moving back and forth.

Primary computational tasks of our DHD for time evolution are to numerically calculate (i) the LU-decomposed matrix \mathbf{A} from the grand resistance matrix \mathbf{R} and (ii) random row vector \mathbf{C} of normal distribution. We used subroutine DPOTRF of LAPACK⁶ for the Cholesky factorization of a real symmetric positive definite matrix \mathbf{R} , and the Box–Muller algorithm to generate normal random numbers for the \mathbf{w} vector.⁷

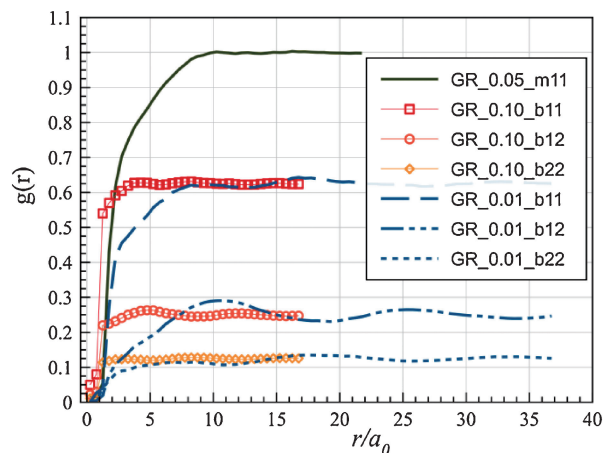


Figure 1. Radial distribution function, $g(r)$, of mono (m)- and bi (b)-dispersed spherical particle suspensions. For bidispersed suspension, big and small particles are indicated using 1 and 2, respectively, and three types of RDF, i.e., g_{11} , g_{12} , and g_{22} , are calculated with volume fractions of 0.01 and 0.1. The radial distance r is scaled by the radius of a monodispersed particle, a_0 .

We tested our new simulation method, DHD, by calculating standard quantities in statistical physics. Figure 1 shows radial distribution functions (RDFs) of mono- and bidispersed spherical particles of volume fraction $\phi = 0.01, 0.05$, and 0.1 . In a cubic simulation box, 1000 particles are initially distributed in a $10 \times 10 \times 10$ array and are randomly shaken to avoid any influences of the initial cubic structure on the calculation (liquid-phase) of the RDFs. Particle sizes have the following relationship: $a_1^3 + a_2^3 = 2a_0^3$, where a_0 is the radius of monodispersed particles, and small and large particle radii are set as $a_2 = 0.750a_0$ and $a_1 = 1.1643a_0$, respectively, for a bidispersed suspension. The volumetric ratio of the big and small particles is therefore 3.7412. The numbers of big and small particles are set to be same in order to maintain the same volume fractions for mono- and bidispersed suspensions. The periodic boundary conditions are applied using an intrinsic FORTRAN function, ANINT, to mimic an infinite medium. Because the hydrodynamic interactions are long-ranged forces, six replicate configurations of the particle suspension are prepared and located on each surface of a cubic simulation box. This Ewald sum technique pushes particles (present near box walls) toward the box center and therefore minimizes statistical inhomogeneity of particle distributions throughout the simulation box. The generalized force \mathbf{Q} is calculated using $7N$ particles, and the size

of the grand mobility matrix, which was inverted at every time step, increased from $6N \times 6N$ to $6(7N) \times 6(7N)$, where 6 indicates the degree of translational/rotational freedom.

The monodispersed hard sphere suspension of low volume fraction 0.05 is simulated first. Figure 1 confirms that the RDF converges to 1.0 if two particles are far from each other ($r \gg a_0$) and vanishes near particle contact.

The RDFs of the bidispersed suspension ($\varphi = 0.01$, blue color) are plotted as the lines indicated as b11 (between big particles, dashed), b12 (between big and small, double-dot-dashed), and b22 (between small ones, dotted). As the interparticle distance increases, RDFs of b11 and b22 show a similar plateau shape and converge to finite values near 0.6 and 0.1, respectively. The RDF b12 shows a (smoothly) curved shape in comparison to b11 and b22, especially near the average distance between two adjacent particles, which is calculated (in general) as twice the maximum length shown for each RDF divided by the cube root of N , i.e., 7.482 for a volume fraction of 0.01. The differences in RDFs' plateau values are attributed to partial volume fractions of big and small particles (with the equal population in this case). While the particles of the different sizes are evenly distributed in low-volume-fraction suspensions, hydrodynamic interactions (sensitive to absolute particle sizes) create a nonplateau shape of b12 because small particles are more strongly influenced by hydrodynamic and volume exclusion forces by big particles.

When volume fraction increases from 0.01 to 0.1, the general trends between b11, b12, and b22 are similar in terms of their converging behavior for large r , but RDFs jump closer to the particle contacts. The RDF of the monodispersed suspension with volume fraction 0.05 resides between those of binary suspension with volume fraction 0.01 and 0.1, before it reaches a plateau. We checked that the sum of three RDFs of binary suspensions (b11, b12, and b22) approaches 1.0 as the radial distance is much longer than particle sizes. In this study, the rigor of the volume exclusion remains at the level of multipole expansions of the hydrodynamic mobility between two unequal-sized spheres. Adding the lubrication interaction was a feasible task although the computational cost significantly increases. When we included the lubrication correction in the hydrodynamic interactions, the grand resistance diverges when any two particles partially overlap each other (this is a conventional problem of SD). To resolve this basic problem, reflecting

boundary conditions can be used before two particles overlap, or dynamically adjustable time step can be a supplementary choice. The later, however, cannot fundamentally resolve the overlap problem because the dimensionless Wiener process, \mathbf{w} , follows a normal distribution so that, in principle, the time step is not a finite constant. The average interparticle distance, based on the volume per particle, can be estimated as $(4\pi/3\varphi)^{1/3}a_0$, which is $7.482a_0$, $4.376a_0$, and $3.473a_0$ for $\varphi = 0.01$, 0.05, and 0.1, respectively. Because the total number of particles is 1000, 10 particles are assigned to each direction on average. Therefore, maximum radial distances shown in Figure 1 are 10 times the average interparticle distances.

We developed a new simulation method, DHD, which is a unified version in terms of the accuracy of hydrodynamic interactions for translation and rotation, and flexibility of the simulation time-step not restricted by the particle relaxation time.

This work is supported by U.S. National Science Foundation (No. CBET04-49431), Korea Institute of Science and Technology Information (No. KSC-20110G2-04), and International Scholar Program of Kyung Hee University, Korea.

Paper based on a presentation made at the International Association of Colloid and Interface Scientists, Conference (IACIS2012), Sendai, Japan, May 13–18, 2012.

References

- 1 M. P. Allen, D. J. Tildesley, *Computer Simulation of Liquids*, Oxford University Press, New York, **1987**.
- 2 D. L. Ermak, J. A. McCammon, *J. Chem. Phys.* **1978**, *69*, 1352.
- 3 P. J. Hoogerbrugge, J. M. V. A. Koelman, *Europhys. Lett.* **1992**, *19*, 155.
- 4 P. Español, P. Warren, *Europhys. Lett.* **1995**, *30*, 191.
- 5 P. Nikunen, M. Karttunen, I. Vattulainen, *Comput. Phys. Commun.* **2003**, *153*, 407.
- 6 E. Anderson, Z. Bai, C. Bischof, S. Blackford, J. Demmel, J. Dongarra, J. Du Croz, A. Greenbaum, S. Hammarling, A. McKenney, D. Sorensen, *LAPACK Users' Guide*, 3rd ed., Society for Industrial and Applied Mathematics, Philadelphia, PA, **1999**.
- 7 G. E. P. Box, M. E. Muller, *Ann. Math. Stat.* **1958**, *29*, 610.